

RSC Advances



This is an *Accepted Manuscript*, which has been through the Royal Society of Chemistry peer review process and has been accepted for publication.

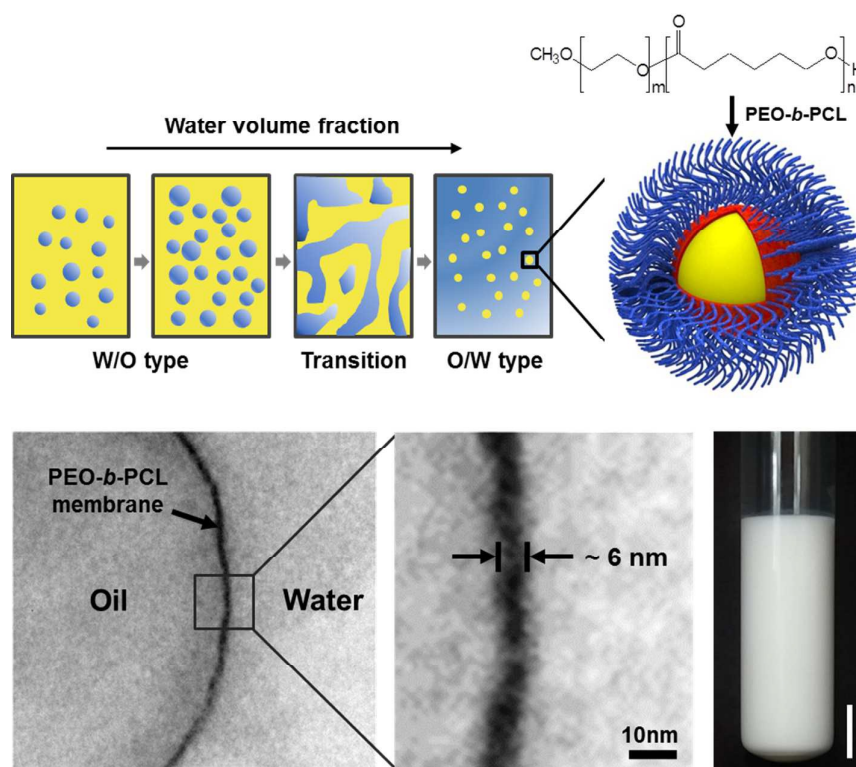
Accepted Manuscripts are published online shortly after acceptance, before technical editing, formatting and proof reading. Using this free service, authors can make their results available to the community, in citable form, before we publish the edited article. This *Accepted Manuscript* will be replaced by the edited, formatted and paginated article as soon as this is available.

You can find more information about *Accepted Manuscripts* in the [Information for Authors](#).

Please note that technical editing may introduce minor changes to the text and/or graphics, which may alter content. The journal's standard [Terms & Conditions](#) and the [Ethical guidelines](#) still apply. In no event shall the Royal Society of Chemistry be held responsible for any errors or omissions in this *Accepted Manuscript* or any consequences arising from the use of any information it contains.

Graphical abstract

Extremely stable O/W nanoemulsions are fabricated by effective assembly of amphiphilic PEO-*b*-PCL copolymer at oil-water interface during phase inversion. The PEO-*b*-PCL forms a thin polymer film at the interface, thereby remarkably improving the emulsion stability.



ARTICLE

Fabrication and stabilization of nanoscale emulsions by formation of thin polymer membrane at oil-water interface

Cite this: DOI: 10.1039/x0xx00000x

Received 00th January 2015,
Accepted 00th January 2015

DOI: 10.1039/x0xx00000x

www.rsc.org/

Kyounghee Shin,^{ab} Jeong Won Kim,^a Hanhee Park,^c Hong Sung Choi,^d
Pil Seok Chae,^a Yoon Sung Nam^{e*} and Jin Woong Kim^{ac*}

This study introduces a robust approach for the fabrication of extremely stable oil-in-water nanoemulsions in which the interface is stabilized by assembly of amphiphilic poly(ethylene oxide)-*block*-poly(ϵ -caprolactone) (PEO-*b*-PCL) copolymers. Phase inversion emulsification, induced by variation of the water volume fraction, facilitated effective assembly of the block copolymers at the oil-water interface. Subsequent application of simple probe-type sonication reduced the droplet size of the precursor emulsions to approximately 200 nm. The prepared nanoemulsions were surprisingly stable against drop coalescence and aggregation, as confirmed by analysis of changes in the droplet size after repeated freeze-thaw cycling and by monitoring the creaming kinetics under conditions of high ionic strength and density mismatch. The results highlight that good structural assembly of the PEO-*b*-PCL block copolymers at the oil-water interface generated a mechanically flexible but tough polymer film, thereby remarkably improving the emulsion stability.

Introduction

Emulsions are a colloidal dispersion system consisting of at least two immiscible liquids, in which one liquid is dispersed as droplets in the other liquid with the aid of emulsifiers. They are thermodynamically unstable, because the separated two phases have the lower free energy than the emulsion itself. Consequently, emulsions always have a tendency toward breakdown over time to reduce the boundary made with unfavourable liquid/liquid contact.¹⁻⁴ The most simple but effective way to resolve this stability issue is to reduce the droplet size. Basically, smaller emulsion droplets provide better dispersion stability against gravitational separation, flocculation and coalescence.⁵⁻⁹ Accordingly, there has been continued interest in the development of nanoscale emulsions, known as nanoemulsions, with typical drop sizes in the range of 20–500 nm.¹⁰⁻¹¹ Thanks to the small drop size, nanoemulsions may prevent sedimentation or creaming, thus possibly offering improved stability. Even in such drop size scales, nonetheless, nanoemulsions are still thermodynamically unstable, due mainly to the Ostwald ripening.^{7,12} The main concern of this study is therefore to develop the nanoemulsion platform technology that can provide the sufficiently long kinetic stability.

The kinetic stability of nanoemulsions can be improved by strengthening the physical property of the oil-water interface. Recently, there have been intense interests in incorporation of amphiphilic block copolymers to emulsion systems as a polymeric

surfactant.¹³⁻¹⁶ They have abilities not only to reduce interfacial tensions at the oil-water interface, but also to form a mechanically stable polymer membrane at the interface. The membrane consisting of the well-designed block copolymers is more resistant to external stresses compared to the typical interface stabilized by small molecular weight surfactants. These unique behaviours of amphiphilic block copolymers allow us to explore a variety of nanoscience applications.¹⁷⁻¹⁸

The general approach for nanoscale emulsions is to input high energy into the system, which ruptures microscale droplets to nanoscale droplets. For this purpose, specialized mechanical devices such as high-pressure homogenizers and ultrasound generators should be commonly utilized.¹⁹⁻²² Alternatively, the incorporation of a large amount of surfactants to the interface reduces the Laplace pressure, thereby leading to production of the smaller droplets. However, there are limits to use such a high concentration of surfactants simply to reduce the droplet size.²³ In this respect, the use of a phase inversion emulsification technique is very attractive, since it can produce stable nanoemulsions with the aid of the chemical energy released during the phase inversion process only.²⁴⁻²⁵ Phase inversion may generally be triggered either by a change in the temperature or composition of the system. These processes are referred to as the phase inversion temperature (PIT) method²⁶⁻³⁰ and the phase inversion composition (PIC) method,^{9,31} respectively. These phase transitions result from changes in the spontaneous curvature of the surfactant. For instance, as the volume of the added

dispersion phase increases, the population of emulsion drops increases to reach a critical packing. At this point, the surfactant molecules exhibit optimal affinity toward each phase, which favours formation of a lamellar liquid crystalline phase or bicontinuous microemulsions. Just above this critical packing volume, phase inversion rapidly occurs.^{23,32-33} Any change in the assembly structure of the surfactant molecules at the phase inversion point affects the interface curvature, which is critical for producing stable nanoemulsions.

In the present study, we introduce a method for producing extremely stable oil-in-water (O/W) nanoemulsions assembled by amphiphilic poly(ethylene oxide)-*block*-poly(ϵ -caprolactone) (PEO-*b*-PCL) copolymers. The originality of our study is to use amphiphilic block copolymers to give the structural membrane stability to the O/W interface. To effectively pack such large molecules at the interface, we employ the PIC method. The phase inversion is induced by dropwise addition of water to the phase consisting of oil, PEO-*b*-PCL, and solvent. PEO-*b*-PCL copolymer used in the proposed emulsion system is distinct in that it forms a thin film at the interface. Various oils are applied in this study. By observing changes in the conductivity of the emulsion system, the phase inversion from a water-in-oil (W/O) emulsion to an O/W emulsion is characterized. Finally, the improved emulsion stability is experimentally evaluated by measuring changes in the droplet size after freeze-thaw cycling and by monitoring the creaming kinetics.

Experimental

Materials

PEO-*b*-PCL copolymers were kindly supplied from ACT (Korea). The measured PCL:PEO ratio was 1.07:1 and the average molecular weight and the polydispersity index were 7.3 kDa and 1.37, respectively. Rapeseed oil, mink oil, and argan oil were generously provided by Natural Solution Co., Ltd. (Korea). Tetrahydrofuran (THF, > 98 %, TCI, Japan) was used as a removable solvent. Olive oil and NaCl were purchased from Samchun Pure Chemical Co., Ltd. (Korea). For all experiments, deionized double distilled water was used.

Preparation of nanoemulsions by using PIC

To prepare primary emulsions, 0.5 g of PEO-*b*-PCL was completely dissolved in 10 mL THF *via* sonication (Power Sonic 510, Hwashin, Korea) for 10 min at 35 °C. This block copolymer solution was miscible with all types of test oils. Subsequently, 2 mL of oil was added to the solution and was vortex mixed. Phase inversion was induced by increasing the volume of water. In each experiment, 8 mL of water was added dropwise to the mixture with vigorous stirring via a syringe pump (Pump 11 Elite, Harvard Apparatus, USA) and the flow rate of water was 100 μ L/min. During optimization of the emulsion composition, the drop size was observed while varying the concentration of PEO-*b*-PCL and oil. Otherwise, the concentrations of PEO-*b*-PCL and oil were kept constant at 5 w/v% and 20 vol%, respectively, relative to the total emulsion volume. In the typical phase inversion procedure, the W/O emulsion formed in a low volume of water was readily converted to

an O/W emulsion at the phase inversion point. The O/W emulsion drops generated after phase inversion had micrometre scale dimensions. THF was completely removed from the system by evaporation at 40 °C. The size of the microscale precursor emulsion was then reduced to the nanoscale by applying strong sonication from a probe-type sonicator (VCX130, Sonic & Materials Inc., USA) equipped with a probe horn of 20 kHz frequency and 130 W. The sonication time was set to 5 min at 60 % amplitude as no further size reduction was observed under these conditions. During sonication, the emulsion container was immersed in a temperature-controlled bath. The temperature was set to 25 °C. This set up could prevent overheating during sonication. The whole process was carried out at room temperature.

Characterization of phase inversion behaviour

Conductivity measurements were conducted to characterize the phase inversion behaviour. The conductivity of the emulsion samples was measured with a conductivity module (856 Module, Metrohm, Switzerland) over the period of water addition at room temperature. The emulsion type (whether O/W or W/O) was decided based on the conductivity of the emulsion system. The volume fraction where the conductivity increased suddenly from 0 μ S/cm was designated as the phase inversion point. The conductivity was measured thrice at each water volume fraction and the average was taken.

Microscopic observation of nanoemulsion drops

The size and morphology of the nanoemulsions were analysed with a transmission electron microscope (TEM, Energy-Filtering Transmission Electron Microscope, LIBRA 120, Carl Zeiss, Germany). The acceleration voltage was 120 kV. A drop of the nanoemulsion sample was placed on a 400 mesh carbon coated copper grid (Ted Pella, Inc., USA). The test sample was negatively stained by using a 1 wt% uranyl acetate solution. The stained sample was completely air-dried prior to TEM observation. The emulsions were also observed with a bright field microscope (NSB-80T, Samwon, Korea).

Evaluation of freeze-thaw emulsion stability

The stability of the emulsion was evaluated by measuring the increase in the average drop size after repeated freeze-thaw cycling. For this evaluation, the vial containing the emulsion was first thoroughly frozen at -20 °C for 12 h in a freezer and then melted at room temperature for 12 h. This freeze-thaw process was repeated at least 5 times. In each freeze-thaw cycle, the size of the emulsion drops was measured by dynamic light scattering (ELS-Z, Otsuka electronics, Japan) using a He-Ne laser with a wavelength of 632.8 nm. The intensity of the scattered light was measured at 173° at 25 °C. To avoid multiple scattering, all samples were diluted with water before measurement.

Observation of creaming kinetics

The emulsion stability was evaluated by investigating the creaming kinetics. To accelerate the creaming velocity of the suspended emulsion drops, the original emulsion was diluted to 10 vol% by adding D₂O. The experiment was then carried out in the presence of

the NaCl, thereby reducing the Debye length, which favours phase separation. 7-mL emulsions containing different amounts of NaCl were prepared and placed in glass tubes. The inner diameter of the tube was 1 cm and the height was 15 cm. The interface generated by creaming was imaged at set time intervals, at room temperature. By comparing the initial height of the emulsion (H_0) against the separated height (H), the creaming kinetics was evaluated. The degree of phase separation was defined as H/H_0 .

Results and discussion

Recent studies on phase inversion and transition state characterization have revealed that control of the phase inversion kinetics is essential for generation of tightly assembled surfactant layers at the interfaces and for production of fine emulsion drops. For instance, when water is added dropwise to the oil phase, the finest O/W emulsion is generated *via* phase inversion. This kinetic control over phase inversion enables uniform assembly of the surfactants at the oil-water interface, thereby accommodating a higher fraction of the internal phase without reversibility of the process by hysteresis.²⁹ Based on earlier studies on phase inversion emulsification, we attempted to produce extremely stable nanoemulsions in which the interface comprises of a well assembled layer of amphiphilic block copolymers, i.e., PEO-*b*-PCL (Fig. 1). PEO-*b*-PCL may give rise to steric repulsion on the surface of the suspended drops due to the hydrophilic PEO block, and can also form a thin polymer membrane due to the hydrophobic PCL block.³⁴

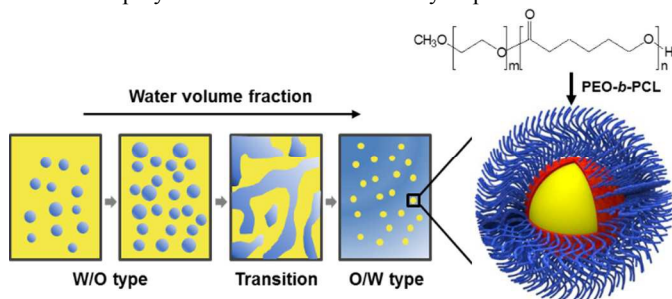


Fig. 1 Schematic of an O/W emulsion formed by phase inversion emulsification. Nanoemulsion drop stabilized with PEO-*b*-PCL is graphically illustrated; the hair corresponds to the PEO chain and the film is formed from PCL.

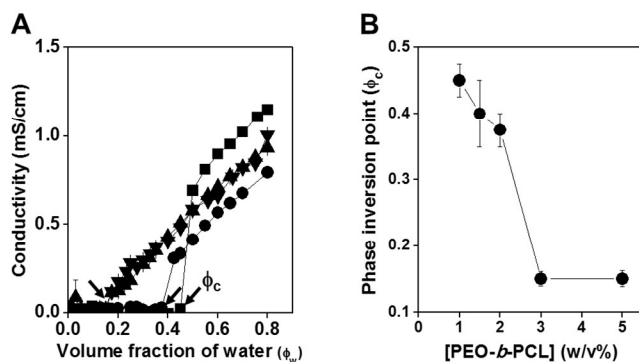


Fig. 2 (A) Change in conductivity as a function of water volume fraction (ϕ_w) during phase inversion at different concentrations of

PEO-*b*-PCL: 1 w/v% (-■-), 2 w/v% (-●-), 3 w/v% (-▲-), and 5 w/v% (-▼-). (B) Dependence of phase inversion point on the concentration of PEO-*b*-PCL. In this experiment, rapeseed oil was used.

For in-depth evaluation of the phase inversion behaviour during emulsification, the conductivity of the continuous phase was measured with the volume fraction of water. Water was added to the oil phase at a flow rate of 100 $\mu\text{L}/\text{min}$. This slow addition of water could provide sufficient time for the block copolymers to be adsorbed on the interface during emulsification. As shown in Fig. 2A, the conductivity was close to 0 $\mu\text{S}/\text{m}$ when the volume fraction of water was low. This indicates that the continuous phase is the oil phase, thus producing a W/O emulsion. At a certain volume fraction of water, the conductivity increased suddenly, because percolation of water drops results in an increase of conductivity due to dynamic droplet clusters or transient water channel.³⁵⁻³⁶ Accordingly, this critical volume fraction of water was designated as the phase inversion point (ϕ_c). ϕ_c depended on the concentration of PEO-*b*-PCL, as shown in Fig. 2B. Increasing the concentration of block copolymers lowered ϕ_c . This indicates that formation of the O/W emulsion is strongly favoured due to the hydrophilic nature of PEO-*b*-PCL, which can be well explained by the Bancroft rule.³⁷ Interestingly, ϕ_c remained constant at ~ 0.16 after the concentration of PEO-*b*-PCL reached 3 w/v%, which is probably associated with the favourable reduction of the interfacial tension at and above the critical concentration of PEO-*b*-PCL.

Before the phase inversion point, semi-transparent water droplets were generated in the continuous oil phase (Fig. 3A). As the volume fraction of water increased, the dispersion became opaque (i.e., milky and white). The viscosity of the continuous phase also increased gradually. At the transition point, the system transformed into a gel-like, highly viscous phase. When this phase was observed using a polarized light microscope, the lamellar liquid crystalline phase could be identified, as shown in Fig. 3B. This observation indicates that the emulsion went through the point of zero curvature in the process of phase inversion. After the phase inversion, oil droplets were dispersed in the aqueous phase (Fig. 3C). Even after removal of THF, no significant difference in the drop size and size distribution was observed (Fig. 3D). This means that the oil drops were well stabilized by PEO-*b*-PCL at the oil-water interface. Notably, after phase inversion, the emulsions obtained herein were of micrometre scale. Generally, when phase inversion emulsification technology is utilized, droplets with sizes less than hundreds of nanometres are obtained. To explain this, we presume that the polymer relaxation time was much longer than the phase transition time. Therefore, the curvature shift of the lamellar phase comprising PEO-*b*-PCL copolymers plausibly occurred on the scale of micrometres.

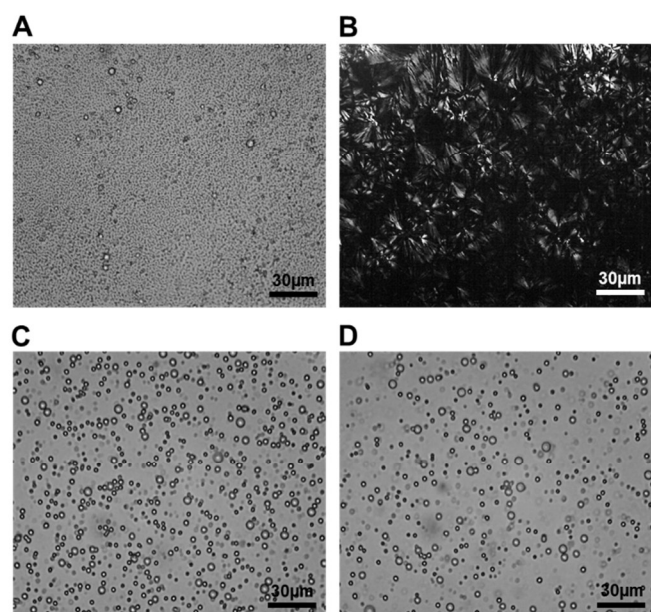


Fig. 3 Optical microscope images of emulsion drops during phase inversion. (A) W/O type emulsion ($\phi_w = 0.07$) before phase inversion. (B) Gel-like lamellar phase ($\phi_w \sim 0.12$) at the phase transition point. (C) O/W type emulsion ($\phi_w \sim 0.8$) after phase inversion. (D) O/W emulsion after removal of THF. For this experiment, we used rapeseed oil.

The size of the droplets in the precursor macroemulsion was reduced by applying probe-type sonication to the emulsion system. Use of the physical stress-driven emulsification technique enabled production of a fine dispersion of nanoemulsion drops. Herein, simple probe sonication for 5 min remarkably reduced the emulsion size to hundreds of nanometres. A representative nanoemulsion produced using an optimized composition was characterized *via* TEM analysis (Fig. 4A). The average droplet sizes for this sample were detected in hundreds of nanometers by dynamic light scattering (Fig. 4B). Considering the hydrodynamic thickness, the difference in the average droplet size based on the two techniques is within reason. From the TEM analysis, we successfully detected the thin PEO-*b*-PCL membrane at the oil-water interface, which is approximately 6 nm (Fig. 4C). The final nanoemulsion was opaque and slightly bluish white (Fig. 4D). Increasing the concentration of PEO-*b*-PCL caused a significant decrease of the droplet size (Fig. 5A). Most importantly, even with the use of a high concentration of oil, the emulsion droplets retained dimensions of hundreds of nanometres (Fig. 5B). To confirm the diversity achievable with the proposed emulsification method, a series of nanoemulsions were produced with different types of oils, including vegetable oils and mineral oils. TEM images of all nanoemulsions are shown in Fig. 6. Irrespective of the type of oils, the emulsion drops could be obtained in dimensions of hundreds of nanometres.

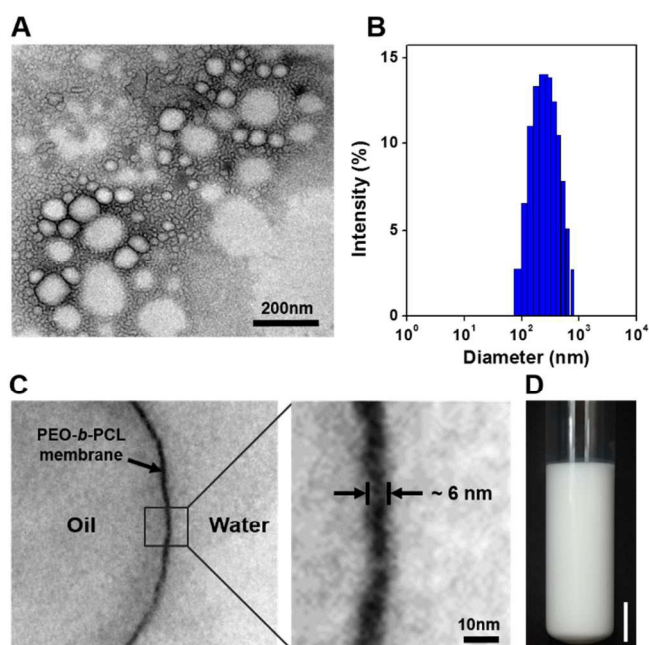


Fig. 4 (A) Transmission electron microscope image of nanoemulsion drops. (B) Size distribution of nanoemulsion drops. (C) Magnified TEM image of PEO-*b*-PCL membrane. (D) Appearance of a nanoemulsion immediately after preparation. This emulsion sample comprised 20 vol% rapeseed oil and 5 w/v% PEO-*b*-PCL. The scale bar is 1 cm.

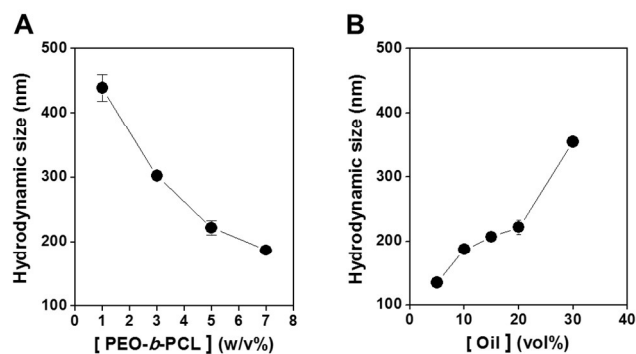


Fig. 5 Average hydrodynamic size of oil droplets. (A) Effect of the concentration of PEO-*b*-PCL. The oil concentration was set to 20 vol% rapeseed oil. (B) Effect of oil concentration. The concentration of PEO-*b*-PCL was set to 5 w/v%.

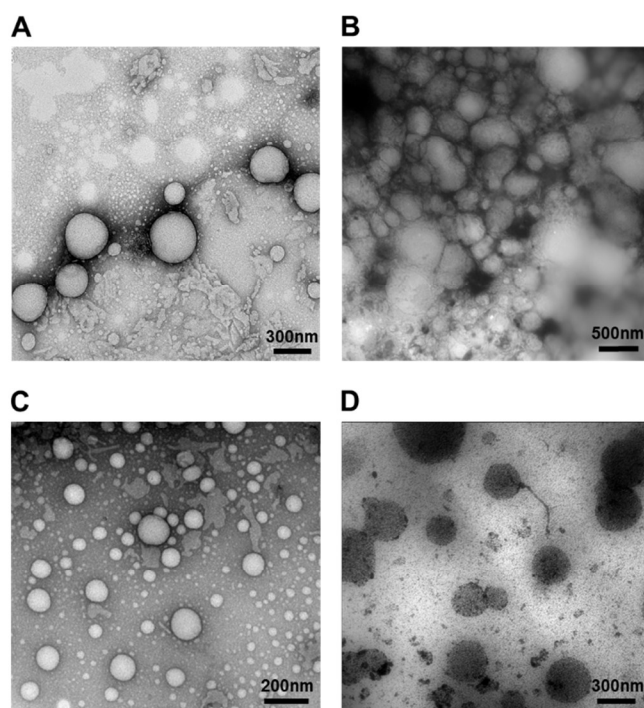


Fig. 6 Transmission electron microscope images of nanoemulsions made with different types of oils: (A) mink oil, (B) argan oil, (C) olive oil, (D) *n*-decane. These emulsions were made with 20 vol% oil and 5 w/v% PEO-*b*-PCL.

To evaluate the stability of the emulsions under harsh conditions, we investigated the effect of pH on the emulsion stability. The emulsion retained excellent dispersion stability over the pH range of 2–12 with no significant phase separation. Furthermore, even in the presence of a large amount of salts (higher than 3 m NaCl), the emulsion also showed the excellent dispersion stability. It is proposed that the obtained results are closely related to the formation of the block copolymer layer at the oil-water interface.³⁸ To exert much stronger mechanical stress and break up the interface, a repeated freeze-thaw test of the emulsions was performed (Fig. 7). As the number of cycles increased, the average droplet size also increased from 200 nm to 500 nm. However, the size remained constant after the several cycle tests. This means that although there was some coalescence because of the repeated freeze-thawing, the emulsions produced in this study showed the tolerance against the mechanical stresses applied. The assembled structure of the block copolymers at the oil-water interface could be affected by the phase inversion kinetics. To confirm this, a control emulsion was produced without employing the phase inversion procedure, in which water was rapidly dumped into the oil phase so that the block copolymer did not have sufficient time to assemble at the interface. In this case, the average droplet size increased markedly to 600 nm from the first cycle and significant elution of oil from the emulsion system could be observed. This adequately demonstrates that to achieve a well assembled block copolymer layer at the interface, phase inversion should be conducted slowly, thus allowing the block copolymer to associate and form the polymer membrane at the oil-water interface.

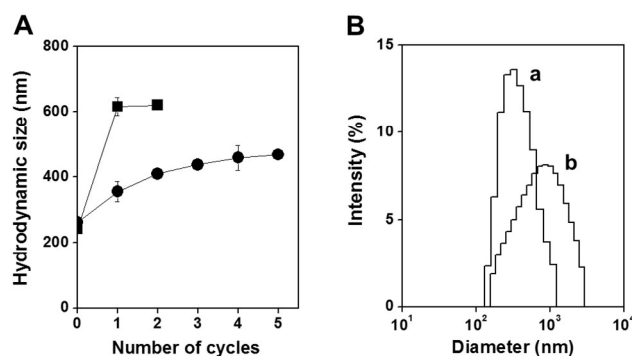


Fig. 7 Evaluation of emulsion stability against freeze-thaw cycling. (A) Evolution of average hydrodynamic size upon repeated freeze-thawing. The emulsions were produced by bulk addition (■) and dropwise addition (●) of water, respectively. (B) Size distributions of nanoemulsion drops after 2 cycles: dropwise addition (a) and bulk addition (b) of water.

As demonstrated by the above results, the nanoemulsion developed in this study was highly stable against mechanical stresses. To further evaluate the emulsion stability, the creaming kinetics was evaluated under harsher conditions, *i.e.* high ionic strength and density mismatch. In principle, the creaming rate (v)³⁹ is expressed as $v \sim \frac{\Delta\rho g a^2}{\eta} (1 - \phi)^{5.5}$, where $\Delta\rho$ is the difference in density between the dispersion phase and continuous phase, g is the gravity, a is the size of the emulsion drop, ϕ is the volume fraction of the emulsion-drop, and η is the viscosity of the emulsion system. Adding NaCl to the emulsion may induce some aggregation of the suspended drops. This can be accelerated by density mismatch. For this purpose, heavy water (90 vol%, D₂O) was introduced into the emulsion, thus increasing $\Delta\rho$. To determine the creaming rate, the height profile of the emulsion samples was recorded during phase separation, as shown in Fig. 8A. As expected, the creaming rate increased as the concentration of NaCl increased. However, the degree of phase separation did not exceed ~ 0.1 , even in the presence of 3 m NaCl after 45 days of storage (Fig. 8B). From this creaming kinetic study, it is evident that the proposed nanoemulsion system is highly stable towards extremes of ionic strength and gravity; this stability originates from generation of a thin block copolymer membrane at the oil-water interface.

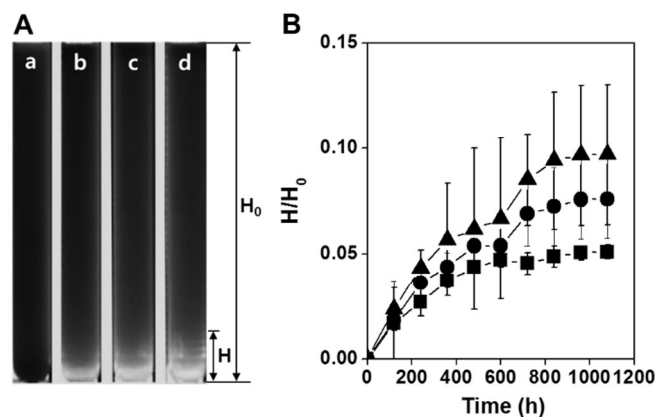


Fig. 8 (A) Phase separation kinetics of nanoemulsions containing different concentrations of NaCl: (a) 0 m (on preparation) (b) 0 m (after 45 days), (c) 1 m (after 45 days), and (d) 3 m (after 45 days). (B) Creaming kinetics of nanoemulsions containing different concentrations of NaCl: 0 m (■), 1 m (●), and 3 m (▲).

Conclusions

This study demonstrated that highly stable nanoemulsions can be fabricated by using the amphiphilic block copolymer, PEO-*b*-PCL. Use of the phase inversion emulsification method facilitated production of microscale precursor emulsions. Simple application of probe-type sonication decreased the drop size to hundreds of nanometres. We have found that manipulation of phase inversion kinetics was critical for generation of a tightly assembled polymer membrane at the interface. The nanoemulsions prepared using this method were highly stable against gravitational force, pH changes, and high ionic strength. The results empirically demonstrate that the structural integrity of the emulsions was maintained under chemical and mechanical stresses. This stability appears to stem from the presence of a thin PEO-*b*-PCL membrane at the oil-water interface. The proposed nanoemulsion system offers great potential for developing a variety of emulsion-based formulations that can not only encapsulate active compounds, but also show tolerance to various environmental factors.

Acknowledgements

This work was supported by a grant of the Korea Healthcare Technology R&D Project, Ministry of Health & Welfare, Republic of Korea (Grant No.: A103017). This research was also supported by the Basic Science Research Program through the National Research Foundation of Korea (NRF) funded by the Ministry of Education, Science and Technology (2012R1A1A2039).

Notes and references

^a Department of Bionano Technology, Hanyang University, Ansan, 426-791, Republic of Korea; Email: kjwoong@hanyang.ac.kr.

^b R&D Center, Nature in Lab. Inc., Gwangju 500-460, Republic of Korea.

^c Department of Applied Chemistry, Hanyang University, Ansan, 426-791, Republic of Korea.

^d Shinsegae International Co. Ltd., Seoul, 135-954, Republic of Korea.

^e Department of Materials Science and Engineering, Korea Advanced Institute of Science and Technology, Daejeon 305-701, Republic of Korea; Email: yoonsung@kaist.ac.kr.

† Footnotes should appear here. These might include comments relevant to but not central to the matter under discussion, limited experimental and spectral data, and crystallographic data.

Electronic Supplementary Information (ESI) available: [details of any supplementary information available should be included here]. See DOI: 10.1039/b000000x/

1. T. F. Tadros and B. Vincent, *Encyclopedia of Emulsion Technology*, Marcel Dekker, New York, 1983.
2. T. F. Tadros, *Emulsion Science and Technology*, Wiley-VCH, Weinheim, 2009.
3. D. J. McClements, *Soft Matter*, 2012, **8**, 1719-1729.
4. J. N.-Nygaard, M. Sletmoen and K. L. Draget, *RSC Adv.*, 2014,

- 4, 52220-52229.
5. T. F. Tadros, P. Izquierdo, J. Esquena and C. Solans, *Adv. Colloid Interface Sci.*, 2004, **108**, 303-318.
6. D. J. McClements, *Soft Matter*, 2011, **7**, 2297-2316.
7. T.G. Mason, J. N. Wilking, K. Meleson, C. B. Chang and S. M. Graves, *J. Phys.: Condens. Matter*, 2006, **18**, R635-R666.
8. H. J. Yang, W. G. Cho and S. N. Park, *J. Ind. Eng. Chem.*, 2009, **15**, 331-335
9. P. Heunemann, S. Prévost, I. Grillo, C. M. Marino, J. Meyere and M. Gradzielski, *Soft Matter*, 2011, **7**, 5697-5710.
10. A. Forgiarini, J. Esquena, C. Gonzalez and C. Solans, *Langmuir*, 2001, **17**, 2076-2083.
11. K. B. Sutradhar and Md. Lutful Amin, *Eur. J. Nanomed.*, 2013, **5**, 97-110.
12. C. Solans, P. Izquierdo, J. Nolla, N. Azemar and M. J. G.-Celma, *Curr. Opin. Colloid Interface Sci.*, 2005, **10**, 102-110.
13. T. J. Barnes and C. A. Prestidge, *Langmuir*, 2000, **16**, 4116-4121.
14. H. K. Cho, J. H. Cho, S.W. Choi, and I. W. Cheong, *J. Microcapsul.*, 2012, **29**(8), 739-746.
15. H. K. Cho, K. S. Cho, J. H. Cho, S. W. Choi, J. H. Kim, and I. W. Cheong, *Colloids Surf. B Biointerfaces*, 2008, **65**, 61-68.
16. H. K. Cho, S. Lone, D. D. Kim, J. H. Choi, S. W. Choi, J. H. Cho, J. H. Kim, and I. W. Cheong, *Polymer*, 2009, **50**, 2357-2364.
17. M. Chausson, A. S. Fluchère, E. Landreau, Y. Aguni, Y. Chevalier, T. Hamaide, N. Abdul-Malak and I. Bonnet, *Int. J. Pharm.*, 2008, **362**, 153-162.
18. K. K. Jette, D. Law, E. A. Schmitt and G. S. Kwon, *Pharm. Res.*, 2004, **21**, 1184-1191.
19. B. Abismail, J. P. Canselier, A. M. Wilhelm, H. Delmas and C. Gourdon, *Ultrasonics Sonochemistry*, 1999, **6**, 75-83.
20. S. Kentish, T. J. Wooster, M. Ashokkumar, S. Balachandran, R. Mawson and L. Simons, *Innovat. Food Sci. Emerg. Tech.*, 2008, **9**, 170-175.
21. S. Debnath, Satayanarayana and G. V. Kumar, *Int. J. Adv. Pharm. Sci.*, 2011, **2**, 72-82.
22. J. G.-Alvarez, D. Boyd, P. Marchal, C. Trebet, P. Perrin, E. M.-Bégué, A. Durand and V. Sadtler, *Colloids Surf. A Physicochem. Eng. Asp.*, 2011, **374**, 134-141.
23. P. Fernandez, V. André, J. Rieger and A. Kähle, *Colloids Surf. A Physicochem. Eng. Asp.*, 2004, **251**, 53-58.
24. S. Shahriar, *Langmuir*, 2006, **22**, 5597-5603.
25. C. Solans and I. Solé, *Curr. Opin. Colloid Interface Sci.*, 2012, **17**, 246-254.
26. K. Shinoda and H. Arai, *J. Phys. Chem.*, 1964, **68**, 3485-3490.
27. K. Shinoda and H. Arai, *J. Colloid Interface Sci.*, 1967, **25**, 429-431.
28. K. Shinoda and H. Saito, *J. Colloid Interface Sci.*, 1968, **26**, 70-74.
29. N. Anton and T. F. Vandamme, *Int. J. Pharm.* 2009, **377**, 142-147.
30. D. Morales, J. M. Gutiérrez, M. J. García-Celma and C. Solans, *Langmuir*, 2003, **19**, 7196-7200.
31. I. Solé, CM. Pey, A. Maestro, C. González, M. Porras and C. Solans et al. *J. Colloid Interface Sci.*, 2010, **344**, 417-23.

32. V. Sadtler, M. R.-Gonzalez, A. Acrement, L. Choplin and E. Marie, *Macromol. Rapid Comm.* 2010, **31**, 998-1002
33. O. Sonnevile-Aubrun, D. Babayan, D. Bordeaux, P. Lindner, Gabriel Ratac and B. Cabaned, *Phys. Chem. Chem. Phys.*, 2009, **11**, 101–110.
34. Y. S. Nam, J. W. Kim, J. Shim, S. H. Han and H. K. Kim, *Langmuir*, 2010, **26** (16), 13038–13043.
35. M. Laguës and C. Sauterey, *J. Phys. Chem.*, 1980, **84**, 3503-3508.
36. S. K. Mehta and K. Bala, *Phys. Rev. E*, 1995, **51**, 5732-5737.
37. W. D. Bancroft, *J. Phys. Chem.*, 1912, **16**, 177-233.
38. H. Park, D. W. Han and J. W. Kim, *Langmuir*, 2015, **31**, 2649-2654.
39. J. J. Lieter-Santos, C. Kim, M. L. Lynch, A. Fernandez-Nieves and D. A. Weitz, *Langmuir*, 2010, **26**, 317.